

Generating Entanglement and Squeezed States of Nuclear Spins in Quantum Dots

M. S. Rudner¹, L. M. K. Vandersypen², V. Vuletić³, L. S. Levitov³

¹ Department of Physics, Harvard University, 17 Oxford St., 5 Cambridge, MA 02138

² Kavli Institute of NanoScience, TU Delft, PO Box 5046, 2600 GA, Delft, The Netherlands

³ Department of Physics, Massachusetts Institute of Technology, 77 Massachusetts Ave, Cambridge, MA 02139

Entanglement generation and detection are two of the most sought-after goals in the field of quantum control. Besides offering a means to probe some of the most peculiar and fundamental aspects of quantum mechanics, entanglement in many-body systems can be used as a tool to reduce fluctuations below the standard quantum limit. For spins, or spin-like systems, such a reduction of fluctuations can be realized with so-called squeezed states¹. Here we present a scheme for achieving coherent spin squeezing of nuclear spin states in few-electron quantum dots. This work represents a major shift from earlier studies in quantum dots, which have explored classical “narrowing” of the nuclear polarization distribution through feedback involving stochastic spin flips^{2–7}. In contrast, we use the nuclear-polarization-dependence of the electron spin resonance (ESR) to provide a non-trivial, area-preserving, “twisting” dynamics¹ that squeezes and stretches the nuclear spin Wigner distribution without the need for nuclear spin flips.

Recently, squeezing of the collective spin state of many atoms was achieved using atom-light or atom-atom interactions^{8–11}. The resulting reduced uncertainty can be used to enhance the performance of atomic clocks, and to achieve unprecedented precision of measurements in atomic ensembles. Similarly, the ability to generate squeezed states in a solid-state setting will open new avenues for quantum control of collective degrees of freedom at the nanoscale. In particular, due to the ubiquity of nuclear spins in nanoscale solid-state devices, future progress in spin-based information processing hinges on our ability to find ways of precisely controlling the dynamics of nuclear spins.

Recently developed experimental techniques provide a powerful toolkit for probing and controlling nanoscale groups of nuclear spins. The electron Zeeman splitting offers a sensitive way to detect the collective nuclear spin polarization through the Overhauser shift of the electronic spin states. This splitting can be measured accurately using spectroscopic or time-domain measurement techniques. Furthermore, the hyperfine coupling provides a means to control the nuclei through their interactions with electron spins. In this way, average nuclear spin polarizations of up to 40% have been achieved¹². Using optical pumping, even larger polarizations of up to 60% have been demonstrated¹³. Fluctuations in one component of the nuclear spin polarization have also been

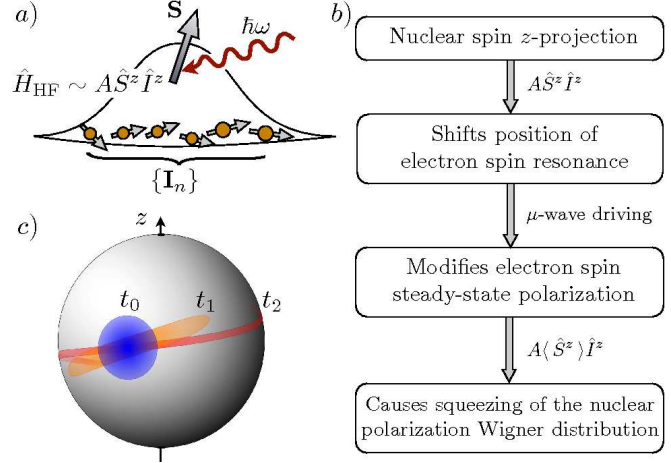


FIG. 1: Nuclear spin squeezing in a quantum dot. a) An electron in a quantum dot, with the electron spin \mathbf{S} coupled to a large group of nuclear spins $\{\mathbf{I}_n\}$. Electron spin resonance is excited by microwave radiation applied in the presence of an external magnetic field. b) Flowchart describing the squeezing mechanism. c) Schematic depiction of twisting dynamics on the Bloch sphere, shown in a rotating frame where the mean polarization is stationary. We focus on short to intermediate times $t_0 \lesssim t \lesssim t_1$, where the phase space (Wigner) distribution is squeezed within a small region of the Bloch sphere, with uncertainty decreasing as $1/t$ beyond the standard quantum limit, Eq.(11). At longer times, indicated by t_2 , the distribution extends around the Bloch sphere, at which point maximal achievable squeezing is reached. For moderate initial nuclear polarizations $p = 2I/N$, significant squeezing can be achieved on the intermediate time scale $t \lesssim t_1$ (see text).

suppressed by a factor of 5-10, by exploiting electron-nuclear feedback^{14–18}. These techniques, together with the possibility of driving coherent nuclear spin rotations using externally applied RF fields^{19–23}, can be used to explore a wide range of quantum phenomena with nuclear spins.

In a system comprised of many spins $\{\hat{\mathbf{I}}_n\}$, such as a quantum dot or an atomic ensemble, the collective total spin $\hat{\mathbf{I}} = \sum_n \hat{\mathbf{I}}_n$ is a quantum mechanical angular-momentum variable. Because different vector components of $\hat{\mathbf{I}}$ do not commute, they are subject to the Heisenberg uncertainty relations

$$\Delta I^y \Delta I^z \geq \frac{\hbar}{2} |\langle \hat{I}^x \rangle|, \quad (1)$$

and its cyclic permutations, where $\Delta I^\alpha = \langle (\delta \hat{I}^\alpha)^2 \rangle^{1/2}$,

with $\delta\hat{I}^\alpha = \hat{I}^\alpha - \langle\hat{I}^\alpha\rangle$. The goal of squeezing is to reduce fluctuations in one spin component below the “quantum limit,” $\Delta I^\alpha = \sqrt{\frac{1}{2}\hbar|\langle\hat{I}^\alpha\rangle|}$, set by Eq.(1) in the situation where the fluctuations are distributed equally between both orthogonal components. Quantitatively, a state is therefore said to be quantum mechanically squeezed along an axis z when the squeezing parameter^{1,24}

$$\xi = \frac{\Delta I^z}{\sqrt{\frac{1}{2}\hbar|\langle\hat{I}^x\rangle|}} \quad (2)$$

is less than one. Because the Heisenberg uncertainty principle must remain satisfied, a reduction of fluctuations ΔI^z signified by $\xi < 1$ must be accompanied by an excess of fluctuations ΔI^y above the quantum limit.

In contrast to the situation in atomic ensembles where classical fluctuations of the collective total spin magnitude \hat{I}^2 can be negligible, however, additional fluctuations in nuclear spin states in quantum dots are unavoidable due to the abundance of nearly degenerate states with energy splittings much smaller than the temperature. Therefore, for typical states in quantum dots, the uncertainty relation (1) is far from being saturated. In a typical situation where the equilibrium state of $N \approx 10^6$ microscopic nuclear spin-1/2 moments is completely random, the classical uncertainties $\Delta I^y = \Delta I^z = \sqrt{N}\hbar/2$ are identical in magnitude to the quantum uncertainty in the maximally polarized (product) state with $\langle\hat{I}^x\rangle = \hbar N/2$, see Eq.(1).³⁰ Below we consider an initial state prepared by polarizing nuclear spins to a fraction p of the maximal polarization, and then rotating this polarization into the equatorial plane of the Bloch sphere such that the mean spin points along x , $\langle\hat{I}^x\rangle_0 = pN\hbar/2$. Because the classical fluctuations in the orthogonal components of the initial state $\Delta I_0^{y,z}$, which are not affected by dynamical nuclear polarization (DNP), are only a factor of $\frac{1}{\sqrt{p}}$ larger than the quantum mechanical minimum fluctuations, $\Delta I^{y,z} \approx \sqrt{pN}\hbar/2$, only a modest amount of additional overhead is required in order to achieve squeezing down to the quantum limit.

We note that, for any mechanism of DNP, the extent of polarization p itself will contain fluctuations. Below we will check, and confirm, that such fluctuations do not present any significant additional challenges for squeezing.

In contrast to recent experiments which achieved spin squeezing through atom-light or atom-atom interactions⁸⁻¹¹, in the mechanism that we outline below, the nuclear spins are driven through their interaction with a single electron spin. As we discuss, the effective squeezing Hamiltonian for nuclei is produced after motional-averaging of the quickly fluctuating, strongly driven electron spin. While the end results (squeezed collective spin states) of these approaches are similar, the physical mechanisms are quite different.

The underlying physics of the feedback mechanism can be understood most easily in the regime of fast dephasing

of the electron spin, which is also a relevant regime for current experimental efforts. As depicted in Fig. 1a, we consider a single electron in a quantum dot, in contact with a large group of nuclear spins, $\{\hat{\mathbf{I}}_n\}$. The electron and nuclear spins are coupled by the hyperfine interaction $H_{\text{HF}} = \sum_n A_n \hat{\mathbf{S}} \cdot \hat{\mathbf{I}}_n$, where $\hat{\mathbf{S}}$ is the electron spin, and each coupling constant A_n is proportional to the local electron density at the position of nucleus n . The electron spin is driven by an applied RF field with frequency close to the electron spin resonance in the presence of an externally applied magnetic field. Because the electron spin evolves rapidly on the timescale of nuclear spin dynamics, the nuclear spins are subjected to an effective hyperfine field (the “Knight field”) produced by the time-averaged electron spin polarization. Feedback results from the dependence of the average electron spin polarization on the detuning from the ESR condition, which in turn depends on the nuclear polarization, see Fig. 1b.

To describe this regime, we model the system with the microscopic Hamiltonian (here and below we take $\hbar = 1$)

$$H = \omega_Z \hat{S}^z + \omega_0 \hat{I}^z + A \hat{I}^z \hat{S}^z + \frac{A}{2} (\hat{I}^+ \hat{S}^- + \hat{I}^- \hat{S}^+) + H_{\text{el}}, \quad (3)$$

where ω_Z is the electron Zeeman energy in the magnetic field, ω_0 is the nuclear Larmor frequency, and H_{el} describes the driving of the electron spin and its coupling to an environment, which leads to fast dephasing and relaxation. For simplicity, here we consider a single species of nuclear spin, and take all hyperfine coupling constants to be equal, $A_n = A$. The latter condition amounts to the assumption that electron density is approximately constant inside the dot, and zero outside. In this case, the electron spin couples directly to the *total* nuclear spin $\hat{\mathbf{I}} = \sum_n \hat{\mathbf{I}}_n$, with the square of the total nuclear spin, \hat{I}^2 , conserved by the dynamics. The effects of non-uniform couplings will be discussed at the end. Due to the large mismatch between the electron and nuclear Zeeman energies, $\omega_Z/\omega_0 \gg 1$, below we ignore the “flip-flop” terms proportional to $\hat{I}^+ \hat{S}^-$ and $\hat{I}^- \hat{S}^+$ in Eq.(3).

We begin by writing the Heisenberg equation of motion for the total nuclear spin operator $\hat{\mathbf{I}}$, $d\hat{\mathbf{I}}/dt = i[\hat{\mathbf{I}}, H]$:

$$\frac{d\hat{\mathbf{I}}}{dt} = \mathbf{b} \times \hat{\mathbf{I}}, \quad \mathbf{b} = (\omega_0 + A \hat{S}^z) \mathbf{z}. \quad (4)$$

When electron dephasing is fast on the characteristic time scale of nuclear spin dynamics, “motional-averaging” allows the electron polarization \hat{S}^z in Eq.(4) to be replaced by an operator-valued semiclassical mean polarization $S^z(\hat{I}^z)$ which depends on the nuclear polarization \hat{I}^z through the Overhauser shift of the ESR frequency, c.f. Ref. 25. In this regime, $S^z(\hat{I}^z)$ is simply determined by rate equations involving the occupation probabilities n_+ , n_- of the up and down electron spin states:

$$\begin{aligned} \dot{n}_- &= W(n_+ - n_-) - \Gamma_1 n_- \\ \dot{n}_+ &= W(n_- - n_+) + \Gamma_1 n_-. \end{aligned} \quad (5)$$

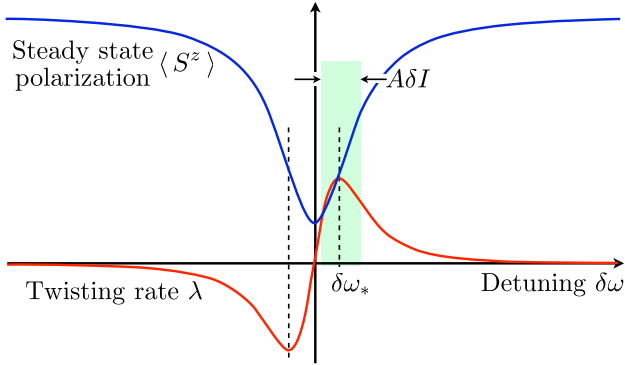


FIG. 2: Time-averaged electron spin polarization S^z , Eq.(6), and squeezing strength λ , Eq.(7), versus RF detuning $\delta\omega$ from the ESR frequency. The average electron spin polarization depends on \hat{I}^z through the dependence of the detuning on the Overhauser shift, as indicated by the shaded region. Squeezing is most efficient for the detuning $\delta\omega_* = \tilde{\gamma}/\sqrt{3}$ where S^z is most sensitive to \hat{I}^z , see text.

Here $W = \frac{1}{2}\Omega^2\gamma/[(\delta\omega - A\hat{I}^z)^2 + \gamma^2]$ is the (\hat{I}^z -dependent) ESR transition rate with detuning $\delta\omega$ between the driving frequency and ω_Z , driving strength Ω , and electron spin dephasing rate $\gamma \equiv 1/T_2$, while Γ_1 is the electron spin relaxation rate. Using this form for W , the steady-state solution of Eq.(5) gives

$$S^z = \frac{1}{2} \frac{(\delta\omega - A\hat{I}^z)^2 + \gamma^2}{(\delta\omega - A\hat{I}^z)^2 + \tilde{\gamma}^2}, \quad \tilde{\gamma}^2 = \gamma^2 + \frac{\gamma}{\Gamma_1}\Omega^2, \quad (6)$$

where $\tilde{\gamma}$ includes the effect of power broadening.

The connection with nuclear spin squeezing is elucidated by linearizing Eq.(6) in $A\hat{I}^z$ around the optimal detuning $\delta\omega_* = \tilde{\gamma}/\sqrt{3}$ where S^z is most sensitive to nuclear polarization-dependent frequency shifts, see Fig.2. Here the nuclear Bloch dynamics described by Eq.(4) can be mapped onto one of the canonical squeezing Hamiltonians proposed by Kitagawa and Ueda¹: absorbing a constant term into the net nuclear Larmor frequency ω_0 , we obtain

$$H \approx \omega_0\hat{I}^z + \frac{1}{2}\lambda(\hat{I}^z)^2, \quad \lambda = A \left. \frac{\partial S^z}{\partial \hat{I}^z} \right|_{\substack{\hat{I}^z=0 \\ \delta\omega=\delta\omega_*}}, \quad (7)$$

with $\hat{I}^2 = I(I+1)$, $I \leq N/2$, conserved by the dynamics.

The squeezing induced by Hamiltonian (7) is most simply illustrated by the evolution of a coherent nuclear spin state of length I initially oriented along x . For large I , semiclassical analysis shows that the quadratic term in Eq.(7) induces precession of the total spin vector about the z axis with a *polarization-dependent* Larmor frequency $\eta = \partial H / \partial I^z = \omega_0 + \lambda I^z$. The resulting evolution has a “twisting” character, in which an area element on the Bloch sphere is stretched in one direction and squeezed in another, see Fig.1c. Squeezing becomes significant at times $t \gtrsim t_S = (|\lambda|I)^{-1}$ when the relative

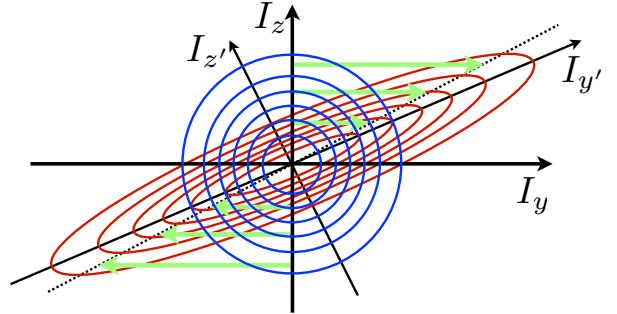


FIG. 3: Contour plot representation of the Wigner distribution of a large collective spin on a locally-flat patch of the Bloch sphere, in the rotating frame where $\omega_0 = 0$. The mean spin points along x . This picture applies for times $t_0 \leq t \leq t_1$, see Fig.1c. Before squeezing, the Wigner distribution is isotropic (blue). After squeezing, the Wigner distribution, Eq.(10), is squeezed along an axis z' , and stretched along an orthogonal axis y' (red). Within the mean-field approximation, phase space area is preserved.

precession between the upper and lower edges of the corresponding “uncertainty region” becomes comparable to the width of the region. Using Eq.(6), and assuming that the spread of Overhauser shifts $A\Delta I^z$ is small compared to the width of the resonance $\tilde{\gamma}$ to ensure the validity of the linearization, we find

$$t_S \approx \frac{16\Gamma_1\tilde{\gamma}^3}{3\sqrt{3}IA^2\gamma\Omega^2}. \quad (8)$$

For an order-of-magnitude estimate of the squeezing time, we set $\Omega = \Gamma_1 = \frac{1}{5}\gamma$. This choice selects the regime of moderately strong electron spin dephasing where the resonance is broader than the minimum value $\gamma = \frac{1}{2}\Gamma_1$. In this practically relevant regime, the rate equations (5) and the motional-averaging approximation can be safely applied. Taking the ‘intrinsic’ width of the resonance to be twice larger than the typical Overhauser field fluctuations, $\gamma \approx A\sqrt{N}$, we obtain

$$t_{S,\min} \approx 20 \frac{\sqrt{N}}{IA}. \quad (9)$$

Using a typical value of the hyperfine coupling for GaAs, $A \approx 0.1 \mu\text{s}^{-1}$, we obtain $t_{S,\min} \approx 200 \mu\text{s}(\sqrt{N}/I)$. The estimate for $t_{S,\min}$ can be improved slightly by optimizing expression (8) with respect to driving power Ω . The fast relaxation rate $\Gamma_1 \sim A\sqrt{N}$ can be achieved by working in a regime of efficient electron spin exchange with the reservoirs in the leads. We see that the squeezing time is inversely proportional to the initial length of the nuclear spin vector, i.e. the degree of nuclear polarization before squeezing.

To investigate the effects of classical fluctuations in the initial state, as well as the effect of time-dependent electron spin fluctuations around the steady state S^z , we now analyze the evolution of the nuclear spin Wigner distribution. For a large initial polarization p , where $I =$

$pN/2$, and for short to intermediate times $t_0 \lesssim t \lesssim t_1$ (see Fig.1c), the “uncertainty region” associated with the nuclear state is small on the scale of the total spin and we can consider evolution in a locally flat patch of the Bloch sphere. Here the operators \hat{I}^y and \hat{I}^z approximately obey canonical commutation relations, and the initial nuclear spin state (polarized along x) is described by an isotropic 2D Gaussian Wigner distribution with width set by the initial transverse fluctuations, $\Delta I \equiv \Delta I_0^{y,z}$. Under the polarization-dependent precession generated by Eq.(7), the Gaussian Wigner distribution evolves to

$$f_t(I^y, I^z) = \mathcal{A} \exp \left(-\frac{(I^z)^2 + (I^y + I\lambda t I^z)^2}{2\Delta I^2} \right), \quad (10)$$

where without loss of generality we set $\omega_0 = 0$. The initial (isotropic) and evolved (squeezed) distributions are shown in Fig.3.

The quadratic form in the exponential in Eq.(10) is diagonalized in a suitably chosen orthonormal basis y' , z' (see Appendix). As shown in Fig.3 and in Eq.(A5), stretching in one direction (y') is accompanied by squeezing in the perpendicular direction (z'), such that the phase space volume of the Wigner distribution is exactly preserved if fluctuations of the electron spin are ignored. For times $t \gtrsim t_S$, see Eq.(8), the uncertainty $\widetilde{\Delta I}$ of the squeezed component decreases as

$$\widetilde{\Delta I}(t) \approx \Delta I \frac{t_S}{t}. \quad (11)$$

Squeezing proceeds until long times when the phase space distribution begins to extend around the Bloch sphere, see Fig.1c. The curvature of the Bloch sphere imposes a limit on the maximum achievable squeezing.¹

To derive the squeezing time t_S in Eq.(8), a coherent nuclear spin state with $\Delta I_{\text{CSS}} = \sqrt{I/2}$ was used. As discussed above, however, when classical uncertainty in the nuclear spin state is included, the initial width of the Wigner distribution is given by $\Delta I = \sqrt{N}/2$. Given that the width $\widetilde{\Delta I}$ of the squeezed component decays as $1/t$, see Eq.(11), the effect of the classical transverse fluctuations is simply to increase the time required to reach a desired level of fluctuations by an order-one factor $\sqrt{N/2I} = \frac{1}{\sqrt{p}}$.

Besides fluctuations in the transverse components of the initial polarization, the DNP process used to prepare the initial nuclear spin state will also leave behind uncertainty in the length I of the net spin (typically with a scale much smaller than I itself). Because Eq.(10) describes *angular precession* with a rate which depends only on the z -component of the total spin, however, sections of the phase space distribution with constant I^z but varying Bloch sphere radii I rigidly precess without growing. Therefore fluctuations in the initial polarization I do not pose a significant threat to squeezing.

In addition to uncertainty in the initial nuclear spin state, we must also consider the effect of time-dependent fluctuations of the electron spin about its mean-field

value S^z , Eq.(6). The mean-field approximation to Eq.(4) applies in the motion-averaged limit when the electron spin evolves quickly on the time scale of the nuclear spin dynamics, and hence the contribution of time-dependent electron spin fluctuations is small. The residual effect of such fluctuations is to add a diffusive component to the nuclear-polarization-dependent precession induced by the time-averaged electron spin. As shown in the Appendix C, the diffusivity κ associated with this phase diffusion approximately goes as $\kappa \sim 1/\Gamma$, where $\Gamma \sim W, \Gamma_1$ is the characteristic rate of electron spin dynamics. Thus phase diffusion is indeed suppressed by motional-averaging when the electron spin evolves quickly on the timescale of nuclear evolution. At long times, the competition between coherent twisting dynamics, which squeezes fluctuations as $1/t$, and phase diffusion, which tends to increase fluctuations as $t^{1/2}$, slows down squeezing to $\widetilde{\Delta I} \sim t^{-1/2}$, but does not prevent it.

The results above are based on a semiclassical mean-field treatment of Eq.(4) supplemented by electron-spin-fluctuation-driven phase diffusion. This intuitive approach is quantitatively supported by a lengthier calculation based on the full density matrix of the combined electron-nuclear system, to be presented elsewhere²⁶. The more powerful density-matrix approach can also be used to study squeezing in the coherent (strong) driving regime of electron spin dynamics where the rate equations, Eq.(5), cannot be applied.

Throughout the discussion, we have worked within the approximation of uniform hyperfine coupling $A_n = A$, see Eq.(3), which is widely used for studying electron-nuclear coupling in quantum dots. More realistically, hyperfine coupling is strong near the center of the dot, where electron density is high, and weak at the edges. We note that similar variations in coupling occur in atomic ensembles when the size of the atom cloud is comparable to the wavelength of light^{9,25}. Squeezing has been demonstrated beautifully in that context, and thus it appears that the variation of couplings does not severely impact the effect.

For achievable polarizations of 20%, squeezing sets in after $t_S \sim 2 \mu\text{s}$, and fluctuations are suppressed by a factor of 10 within approximately 20 μs (neglecting phase diffusion). Due to classical fluctuations in the initial state, first $\frac{1}{\sqrt{p}}$ -fold squeezing goes toward reaching the standard quantum limit, after which quantum squeezing proceeds. These timescales are 10 – 100 times shorter than the approximately 1 ms-scale nuclear coherence time recently measured in vertical double quantum dots²³. It should thus be possible to squeeze the nuclear spin state faster than it decoheres.

All elements required for achieving and demonstrating squeezing have been realized experimentally in nanostructures at low temperature. Dynamical nuclear polarization can routinely be produced¹² and controllably rotated using NMR pulses^{19–23}, and the degree of squeezing can be ascertained through electron spin dephasing measurements^{14,18,27,28}. Furthermore, electron spin res-

onance has been achieved by excitation using microwave magnetic fields, with driving amplitudes comparable to the random nuclear field acting on the electron spin, $A\delta I$.²⁹ The corresponding transition rates W are of the order of 10 MHz. In order to reach the motional averaging regime, the electron spin relaxation rate, Γ_1 , must be comparable to the transition rate W , which can be easily accomplished by allowing cotunneling to the electron reservoirs next to the dot.

In summary, squeezed states of nuclear spins can be produced in quantum dots via feedback provided by their hyperfine coupling to an electron spin driven close to resonance. We have considered various physical effects that compete with squeezing, and estimated the timescale of squeezing. Our estimates indicate that squeezing is feasible and can be realized with current capabilities. The squeezing mechanism, based on microwave driving of the electron spin, can also be easily adapted to the case of optically controlled quantum dots, where resonant Raman transitions are used to drive single electron spins. Such schemes open the door to unprecedented levels of quantum control over collective degrees of freedom in nanoscale systems with mesoscopic numbers 10^4 to 10^6 of nuclear spins.

We thank M. D. Lukin and the Delft spin qubit team for useful discussions. LV acknowledges the MIT Condensed Matter Theory group for its hospitality. This work was supported by the Dutch Foundation for Fundamental Research on Matter and a European Research Council Starting Grant (LV), the NSF-funded MIT-Harvard Center for Ultracold Atoms (LV and VV), the NSF grants DMR-090647 and PHY-0646094 (MR) and PHY-0855052 (VV).

Appendix A: Squeezing of the Wigner Distribution

In this section, we provide a mathematical description of squeezing by analyzing the evolution of a nuclear spin state characterized by a Gaussian Wigner distribution. As discussed in the main text, for a large spin initially oriented in the x direction, and for short times before the Wigner distribution extends significantly around the Bloch sphere, the Wigner distribution in a locally flat patch of Bloch sphere evolves as $f_t(I_y, I_z) = \mathcal{A}e^{-\frac{1}{2}\mathbf{v}^T Q \mathbf{v}}$, see Eq.(10), with

$$\mathbf{v} = \begin{pmatrix} I^y \\ I^z \end{pmatrix}, \quad Q = \frac{1}{\Delta I^2} \begin{pmatrix} 1 & \lambda It \\ \lambda It & 1 + (\lambda It)^2 \end{pmatrix}. \quad (\text{A1})$$

Here $\Delta I = \Delta I_0^{y,z}$ characterizes the transverse fluctuations in the initial nuclear spin state.

For times $t > 0$, the circular Wigner distribution is deformed to an ellipse, with major and minor axes determined by the quadratic form Q in Eq.(A1). As shown in Fig.3 of the main text, stretching in one direction (y') is accompanied by squeezing in the perpendicular direction (z'), such that the phase space volume of the Wigner distribution is preserved. The major and minor axes y' and

z' , which lie parallel to the eigenvectors of Q , are rotated relative to y and z by an angle θ :

$$\begin{pmatrix} I^{y'} \\ I^{z'} \end{pmatrix} = \begin{pmatrix} \cos \theta & -\sin \theta \\ \sin \theta & \cos \theta \end{pmatrix} \begin{pmatrix} I^y \\ I^z \end{pmatrix}. \quad (\text{A2})$$

The angle θ can be found by extremizing the quantity

$$W = \mathbf{w}_\theta^T Q \mathbf{w}_\theta, \quad \mathbf{w}_\theta = \begin{pmatrix} \cos \theta \\ -\sin \theta \end{pmatrix} \quad (\text{A3})$$

with respect to θ . Using the identity $[1 - \tan^2 \theta]/2 \tan \theta = \cot 2\theta$, we find

$$\cot 2\theta = \lambda It/2. \quad (\text{A4})$$

Note that Eq.(A4) has two solutions $\theta_{1,2}$ separated by 90° , as expected for a symmetric form.

In the eigenbasis, we write

$$f_t(I^{y'}, I^{z'}) = \mathcal{A} \exp \left[-\frac{1}{2} \left(\frac{I^{y'}}{\Delta I_+(t)} \right)^2 - \frac{1}{2} \left(\frac{I^{z'}}{\Delta I_-(t)} \right)^2 \right], \quad (\text{A5})$$

with

$$\Delta I_\pm^2(t) = \Delta I^2 \left(1 + \frac{(\lambda It)^2}{2} \left[1 \mp \sqrt{1 + \frac{4}{(\lambda It)^2}} \right] \right)^{-1}. \quad (\text{A6})$$

In the long time limit $\lambda It \gg 1$, the width $\widetilde{\Delta I}(t) \equiv \Delta I_-(t)$ of the squeezed component reduces to Eq.(11).

Appendix B: Phase Diffusion

The effect of time-dependent fluctuations of electron spin polarization about the mean field value can be analyzed within the rate equation model by introducing a time-dependent quantity

$$\tilde{S}^z(t) = S^z + \delta S^z(t). \quad (\text{B1})$$

The fluctuating part δS^z can be modeled as delta-correlated noise $\langle \delta S^z(t') \delta S^z(t'') \rangle \propto \delta(t' - t'')$, with an intensity determined by the rate process, Eq.(5). As shown in Supplementary Section C, such noise generates phase diffusion,

$$\langle \delta \theta^2(t) \rangle = \kappa t, \quad \kappa = 2A^2 \frac{(W + \Gamma_1)W}{(2W + \Gamma_1)^3}, \quad (\text{B2})$$

where $\delta \theta$ is the fluctuating part of the Larmor precession angle, $I^x + iI^y \propto e^{i(\theta + \delta \theta)}$. The phase diffusion can be accounted for by adding a diffusion term with diffusivity $\tilde{\kappa} = I^2 \kappa$ to the equation describing the time evolution of the Wigner distribution.

An important consequence of phase diffusion is non-conservation of phase volume, which can be illustrated

by the evolution of a Gaussian Wigner distribution. Similar to the mean-field case, Eq.(10), such a distribution evolves in time as

$$f_t(I^y, I^z) = \mathcal{A}'(t) \exp \left[-\frac{(I^z)^2}{2\Delta I^2} - \frac{(I^y + I\lambda t I^z)^2}{2(\Delta I^2 + \tilde{\kappa}t)} \right], \quad t > 0. \quad (\text{B3})$$

Initially, phase diffusion leads to a broadening of the Wigner distribution, characterized by the factor $\sqrt{1 + \tilde{\kappa}t/\Delta I^2}$, which grows like $t^{1/2}$ for $\tilde{\kappa}t > \Delta I^2$. At later times, $\Delta I \lambda t I \gtrsim \sqrt{\tilde{\kappa}t}$, the behavior is dominated by the linear in t twisting/stretching dynamics. Therefore for times satisfying $t > t_{\text{noise}} = \frac{2A^2\kappa}{N\lambda^2}$, the coherent stretching overwhelms the effect of phase diffusion.

The efficiency of squeezing in the presence of phase diffusion can be estimated as follows. At long times $t \gg t_{\text{noise}}$, the factor $\sqrt{1 + \tilde{\kappa}t/\Delta I^2}$ describes an increase of the width of the Wigner distribution compared to its ideal squeezed value ΔI in Eq.(11). Combining the $t^{1/2}$ smearing due to phase diffusion with the t^{-1} squeezing, we find that the width of the Wigner distribution decreases as $t^{-1/2}$ at long times:

$$\widetilde{\Delta I}_{\text{noise}} = \widetilde{\Delta I}(t) \sqrt{1 + \tilde{\kappa}t/\Delta I^2} \approx \frac{\tilde{\kappa}^{1/2}}{\lambda I} t^{-1/2} \quad (\text{B4})$$

This expression describes the slowing of squeezing due to phase diffusion.

Appendix C: Calculation of the Phase Diffusion Constant

To analyze phase diffusion, we need to calculate the generating function for spin fluctuations driven by up-down and down-up switching. Denoting the two switching rates as W and W' , we can obtain the generating function for spin fluctuations during the time interval $0 < t' < t$ by approximating a continuous Poisson process by a discrete Markov process with a small time step $\Delta \ll W^{-1}, (W')^{-1}, t$. We have

$$\chi(\lambda) = \begin{pmatrix} 1 \\ 1 \end{pmatrix}^T \left[e^{i\Delta(\lambda/2)\sigma_3} R_\Delta \right]^N \begin{pmatrix} 1/2 \\ 1/2 \end{pmatrix} \quad (\text{C1})$$

$$R_\Delta = \begin{pmatrix} 1 - W\Delta & W\Delta \\ W'\Delta & 1 - W'\Delta \end{pmatrix}, \quad N = \frac{t}{\Delta},$$

where $W' = W + \Gamma_1$. Taking the limit $\Delta \rightarrow 0$, $N \rightarrow \infty$ we obtain an expression

$$\chi(\lambda) = \begin{pmatrix} 1 \\ 1 \end{pmatrix}^T e^M \begin{pmatrix} 1/2 \\ 1/2 \end{pmatrix}, \quad (\text{C2})$$

$$M = t \begin{pmatrix} i\lambda/2 - W & W \\ W' & -i\lambda/2 - W' \end{pmatrix}. \quad (\text{C3})$$

The generating function (C2) provides a full description of the statistics of phase fluctuations, $\theta_t = \int_0^t S_Z(t) dt$, by encoding all its cumulants:

$$\ln \chi(\lambda) = \sum_{k=1}^{\infty} m_k \frac{(i\lambda)^k}{k!}, \quad (\text{C4})$$

with m_1 and m_2 giving the expectation value $\langle S_z \rangle t$ and the variance $\langle (\theta_t - \langle \theta_t \rangle)^2 \rangle$, respectively. The latter quantity yields the phase diffusion constant via $m_2 = \kappa t$.

Matrix exponential e^M can be evaluated by writing it in terms of Pauli matrices, $M = x_0 + x_i \sigma_i$, where

$$x_0 = -W_+, \quad x_1 = W_+, \quad x_2 = iW_-, \quad x_3 = i\lambda/2 - W_-, \quad (\text{C5})$$

and we defined $W_{\pm} = (W \pm W')/2$. We have

$$e^M = e^{x_0 t} \left(\cosh(Xt) + \frac{\sinh(Xt)}{X} x_i \sigma_i \right) \quad (\text{C6})$$

where $X^2 = x_1^2 + x_2^2 + x_3^2 = W_+^2 - \lambda^2/4 - i\lambda W_-$. Plugging this expression for e^M in Eq.(C2), we find

$$\chi(\lambda) = 2e^{x_0 t} \left(\cosh(Xt) + \frac{\sinh(Xt)}{X} x_1 \right), \quad (\text{C7})$$

an exact expression which is valid both at short times and at long times.

To analyze fluctuations in the steady state, we focus on the long times $t \gg W^{-1}, (W')^{-1}$. In this limit, the behavior of $\chi(\lambda)$ can be understood by replacing $\cosh Xt$ and $\sinh Xt$ by e^{Xt} , giving

$$\ln \chi(\lambda) \approx (X - W_+)t = -\frac{\lambda^2/4 + i\lambda W_-}{X + W_+} t \quad (\text{C8})$$

Taylor expanding this expression up to order λ^2 we find the first and second cumulants of phase fluctuations:

$$\ln \chi(\lambda) = -i\lambda \frac{W_- t}{2W_+} + \frac{(i\lambda)^2}{2} \frac{(W_+^2 - W_-^2)t}{4W_+^3} + O(\lambda^3) \quad (\text{C9})$$

Substituting $W' = W + \Gamma_1$, we obtain the time-averaged polarization and the phase diffusion constant

$$\langle S_z \rangle = \frac{1}{2} \frac{\Gamma_1}{2W + \Gamma_1}, \quad \kappa = 2 \frac{(W + \Gamma_1)W}{(2W + \Gamma_1)^3} \quad (\text{C10})$$

Crucially, the phase diffusion slows down when the switching rates W and W' grow, which justifies our motional averaging approximation.

¹ Kitagawa, M. & Ueda, M. Squeezed spin states, Phys. Rev. A 47, 5138 (1993)

² Klauser, D., Coish, W. A. & Loss, D. Nuclear spin state

narrowing via gate-controlled Rabi oscillations in a double quantum dot, *Phys. Rev. B* **73**, 205302 (2006)

³ Giedke, G., Taylor, J. M., D'Alessandro, D., Lukin, M. D., & Imamoglu, A. Quantum measurement of a mesoscopic spin ensemble, *Phys. Rev. A* **74**, 032316 (2006)

⁴ Stepanenko, D., Burkard, G., Giedke, G. & Imamoglu, A. Enhancement of electron spin coherence by optical preparation of nuclear spins, *Phys. Rev. Lett.* **96**, 136401 (2006)

⁵ Rudner, M. S. & Levitov, L. S. Self-Polarization and Dynamical Cooling of Nuclear Spins in Double Quantum Dots, *Phys. Rev. Lett.* **99**, 036602 (2007)

⁶ Rudner, M. S. & Levitov, L. S. Dynamical Cooling of Nuclear Spins in Double Quantum Dots, *Nanotechnology* **21**, 274016 (2010)

⁷ Danon, J. & Nazarov, Yu. V., Nuclear tuning and detuning of the electron spin resonance in a quantum dot: Theoretical consideration, *Phys. Rev. Lett.* **100**, 056603 (2008)

⁸ Appel, J., Windpassinger, P., Oblak, D., Hoff, U., Kjaergaard, N. & Polzik, E. S. Mesoscopic atomic entanglement for precision measurements beyond the standard quantum limit, *Proc. Natl. Acad. Sci. USA* **106**, 10960 (2009)

⁹ Schleier-Smith, M. H., Leroux, I. D., & Vuletić, V. States of an Ensemble of Two-Level Atoms with Reduced Quantum Uncertainty, *Phys. Rev. Lett.* **104**, 073604 (2010).

¹⁰ Gross, C., Zibold, T., Nicklas, E., Estève, J. & Oberthaler, M. K. Nonlinear atom interferometer surpasses classical precision limit, *Nature* **464**, 1165 (2010).

¹¹ Riedel, M. F., Böhi, P., Li, Y., Hänsch, T. W., Sinatra, A. & Treutlein, P. Atom-chip-based generation of entanglement for quantum metrology, *Nature* **464**, 1170 (2010).

¹² Baugh, J., Kitamura, Y., Ono, K. & Tarucha, S. Large nuclear Overhauser fields detected in vertically coupled double quantum dots, *Phys. Rev. Lett.* **99**, 096804 (2007).

¹³ Bracker, A. S., Stinaff, E. A., Gammon, D., Ware, M. E., Tischler, J. G., Shabaev, A., Efros, Al. L., Park, D., Gershoni, D., Korenev, V. L. & Merkulov, I. A. Optical Pumping of the Electronic and Nuclear Spin of Single Charge-Tunable Quantum Dots, *Phys. Rev. Lett.* **94**, 047402 (2005)

¹⁴ Geilich, A., Spatzek, S., Yugova, I. A., Akimov, I. A., Yakovlev, D. R., Efros, Al. L., Reuter D., Weick, A. D. & Bayer, M. Collective single-mode precession of electron spins in an ensemble of singly charged (In,Ga)As/GaAs quantum dots, *Phys. Rev. B* **79**, 201305(R) (2009).

¹⁵ Vink, I. T., Nowack, K. C., Koppens, F. H. L., Danon, J., Nazarov, Yu. V. & Vandersypen, L. M. K. Locking electron spins into magnetic resonance by electron-nuclear feedback, *Nature Physics* **5**, 764 (2009).

¹⁶ Latta, C., Högele, A., Zhao, Y., Vamivakas, A. N., Maletinsky, P., Kroner, M., Dreiser, J., Carusotto, I., Badolato, A., Schuh, D., Wegscheider, W., Atature, M. & Imamoglu, A. Confluence of resonant laser excitation and bidirectional quantum-dot nuclear-spin polarization, *Nature Physics* **5**, 758 (2009)

¹⁷ Xu, X., Yao, W., Sun, B., Steele, D. G., Bracker, A. S., Gammon, D. & Sham, L. J. Optically controlled locking of the nuclear field via coherent dark-state spectroscopy, *Nature* **459**, 1105 (2009).

¹⁸ Bluhm, H., Foletti, S., Mahalu, D., Umansky, V. & Yacoby, A. Enhancing the Coherence of Spin Qubits by Narrowing the Nuclear Spin Bath Using a Quantum Feedback Loop, *Phys. Rev. Lett.* **105**, 216803 (2010).

¹⁹ Machida, T., Yamazaki, T. & Komiyama, S. Local control of dynamic nuclear polarization in quantum Hall devices, *Appl. Phys. Lett.* **80**, 4178 (2002)

²⁰ Machida, T., Yamazaki, T., Ikushima, K., & Komiyama, S. Coherent control of nuclear-spin system in a quantum-Hall device, *Appl. Phys. Lett.* **82**, 409 (2003)

²¹ Yusa, G., Muraki, K., Takashina, K., Hashimoto, K. & Hirayama Y. Controlled multiple quantum coherences of nuclear spins in a nanometre-scale device, *Nature* **434**, 1001 (2005)

²² Tartakovskii group, private communication.

²³ Takahashi, R., Kono, K., Tarucha, S. & Ono, K. Reversible Nuclear Spin Polarization Selected by Voltage in Semiconductor Quantum Dot Devices, arXiv:1012.4545 (2010).

²⁴ Wineland, D. J., Bollinger, J. J., Itano, W. M. & Heinzen, D. J. Squeezed atomic states and projection noise in spectroscopy, *Phys. Rev. A* **50**, 67 (1994).

²⁵ Schleier-Smith, M. H., Leroux, I. D., & Vuletić, V. Squeezing the collective spin of a dilute atomic ensemble by cavity feedback, *Phys. Rev. A* **81**, 021804(R) (2010).

²⁶ Rudner, M. S., Levitov, L. S. & Vandersypen, L. M. K., in preparation (2011).

²⁷ Petta, J. R., Johnson, A. C., Taylor, J. M., Laird, E. A., Yacoby, A., Lukin, M. D., Marcus, C. M., Hanson, M. P. & Gossard, A. C. Coherent Manipulation of Coupled Electron Spins in Semiconductor Quantum Dots, *Science* **309**, 2180 (2005)

²⁸ Koppens, F. H. L., Nowack, K. C. & Vandersypen, L. M. K. Spin Echo of a Single Electron Spin in a Quantum Dot, *Phys. Rev. Lett.* **100**, 236802 (2008)

²⁹ Koppens, F. H. L., Buijzer, C., Tielrooij, K. J., Vink, I. T., Nowack, K. C., Meunier, T., Kouwenhoven, L. P. & Vandersypen, L. M. K. Driven coherent oscillations of a single electron spin in a quantum dot, *Nature* **442**, 766 (2006)

³⁰ For simplicity we consider microscopic spins of size $s = 1/2$, but the generalization to other spins is straightforward.